Wind Stress Measurements from the Open Ocean

MARGARET YELLAND AND PETER K. TAYLOR

James Rennell Division for Ocean Circulation, Southampton Oceanography Centre, Southampton, United Kingdom

(Manuscript received 1 May 1995, in final form 1 September 1995)

ABSTRACT

An automatic inertial dissipation system was used during three cruises of the RRS *Discovery* in the Southern Ocean to obtain a large dataset of open ocean wind stress estimates. The wind speed varied from near calm to 26 m s^{-1}, and the sea–air temperature differences ranged from −15° to +7°C. The data showed that the assumption of a balance between local production and dissipation of turbulent kinetic energy is false and that the sign and magnitude of the imbalance depends critically on both stability and wind speed. The wide range of stability conditions allowed a new formulation for the nondimensional dissipation function under diabatic conditions.

A minimum in the 10-m neutral value of the drag coefficient occurred at 6 m s^{-1}. At lower wind speeds the data were fitted by the relationship

$$1000C_{D10n} = 0.29 + \frac{3.1}{U_{10n}} + \frac{7.7}{U_{10n}^2} \quad (3 \leq U_{10n} \leq 6 \text{ m s}^{-1}),$$

where U_{10n} is the 10-m neutral wind speed (m s^{-1}). At higher wind speeds

$$1000C_{D10n} = 0.60 + 0.070 * U_{10n} \quad (6 \leq U_{10n} \leq 26 \text{ m s}^{-1}),$$

which gives drag coefficients that are about 10% higher than those from previous open ocean studies (which assumed a balance between production and dissipation). Wave measurement suggested that the sea state was not, on average, fully developed at wind speeds above 15 m s^{-1}. However, contrary to findings from other studies, no large anomalies in the drag coefficient were detected despite the range of conditions and sea states encountered. It is believed that the ideal conditions (such as the absence of swell) needed to detect the effects of sea state on the wind stress may occur rather infrequently over the open ocean.

1. Introduction

This paper presents sea surface wind stress determinations over a wide range of wind speeds obtained using the inertial dissipation method from deep ocean, long fetch regions of the Southern Ocean. This large dataset is also used to determine the form of the nondimensional dissipation function under diabatic conditions.

The sea surface wind stress is important because it creates the surface wave field and drives the ocean circulation. Realistic modeling of the atmospheric and oceanic boundary layers, and of the surface wave field, depends on the correct specification of the surface drag coefficient (e.g., Geernaert 1987). Although the variation of wind stress with wind speed and sea state has been a continuing subject of research for many years, most data has been collected at nearshore, shallow water sites. However, it has been demonstrated (Geernaert et al. 1987) that, due to the modification of the waves, higher wind stress values occur for a given wind speed in shallow water. In the survey of Blanc (1985) or the review of Donelan (1990) the main open ocean datasets remain those of Smith (1980) and Large and Pond (1981), both based on the use of the same Bedford Institute of Oceanography (BIO) tower facility. The amount of data collected in deep water, open ocean conditions has been limited because the use of the eddy correlation method for determining wind stress is impractical on a ship, mainly due to the airflow disturbance caused by the ship's superstructure. To avoid this problem, Smith (1980) implemented the BIO tower, a taut moored spar buoy, and obtained eddy correlation wind stress estimates using a thrust anemometer. During the same experiment, Large and Pond (1981, 1982) demonstrated that wind stress estimates using the inertial dissipation method were, under most conditions, equivalent to the eddy correlation data. They then extended their dataset using the inertial dissipation method with data collected from research ships operating in open ocean areas.

Comparisons of the inertial-dissipation method against eddy correlation data over the sea have been

Corresponding author address: Miss Margaret J. Yelland, James Rennell Division for Ocean Circulation, Southampton Oceanography Centre, Empress Dock, Southampton SO14 3ZH, United Kingdom.

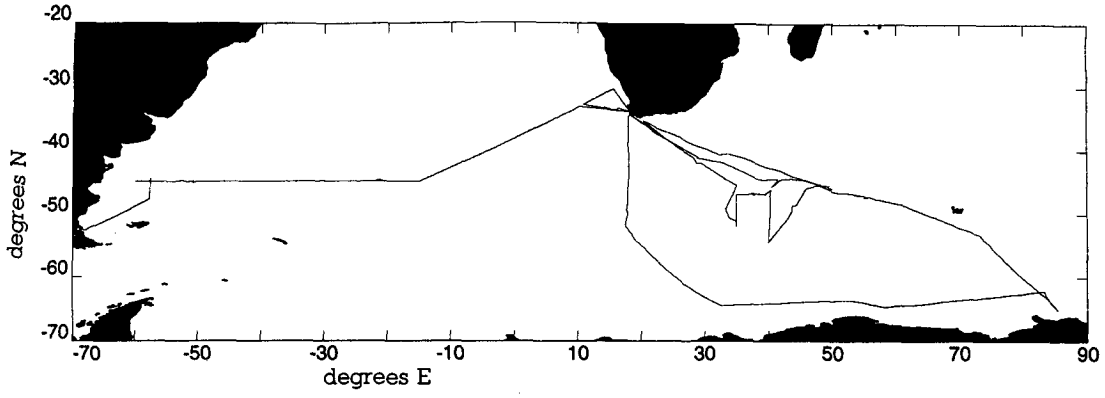

FIG. 1. RRS *Discovery* Southern Ocean track plot.

reported by various authors (Dunckel et al. 1974; Schmitt et al. 1978; Geernaert et al. 1988; Edson et al. 1991). The inertial dissipation method has been found to be less affected by airflow disturbance about the measuring platform compared to the eddy correlation method (Edson et al. 1991). In addition, the eddy correlation method requires a large sample time, which depends on both wind speed and measurement height (Wyngaard 1973), during which conditions must be stationary. Most eddy correlation studies over the ocean have used sampling periods of between 30 minutes and one hour in an attempt to ensure that all scales of momentum transferring eddies are properly sampled. On the other hand, the inertial dissipation method only requires a sampling period sufficient to determine the spectral density within the inertial subrange, that is, at frequencies of a few hertz. Sampling periods of 20 minutes or less are commonly used; Marsden et al. (1993) successfully employed a sampling period of 1 minute. Although Large and Businger (1988) and Fairall et al. (1990) have described automatic instrumentation systems for routine inertial dissipation wind stress estimation on ships, the number of instrument deployments in the deep ocean has remained low. Indeed, prior to the data reported in this paper, Large and Pond (1982) has remained the major wind stress dataset.

During three cruises of the research ship RRS *Discovery* in the Southern Ocean, an automatic inertial dissipation system, similar to that used by Yelland et al. (1994), collected a large dataset of open ocean inertial-dissipation wind stress estimates. The measurement method and derivation of the wind stress will be described in section 2. The data obtained are the first measurements reported from the Southern Ocean, an area characterized by large swell waves and well-developed seas. During the cruises, wind speeds ranged from near calm to 26 m s^{-1}; sea–air temperature differences ranged from −15° to +7°C. This wide range of stability conditions has both necessitated and enabled a new formulation for the nondimensional dissipation function under diabatic conditions (section 3). An independent test of this formulation will be presented using data from the SOFIA experiment. During this experiment, the French Research Ship *le Suroit* operated off the Azores, which in terms of climate is a significantly different ocean area than the Southern Ocean. Having corrected the data for stability effects, the wind stress, drag coefficient, and wind speed relationships will be discussed in section 4. The Southern Ocean data significantly increase the number of open ocean wind stress estimates available at gale force and higher wind speeds, and they improve our knowledge of the behavior of the drag coefficient at low wind speeds. The results will be summarized in section 5.

2. The inertial dissipation method

a. Theoretical background

The inertial dissipation method has been reviewed by Fairall and Larsen (1986) and has recently received detailed evaluation by Edson et al. (1991). However, different options exist for implementing the method, and these may significantly affect the results, particularly with regard to the form of the nondimensional dissipation function. Thus, it is necessary to describe the specific equations and implementation method that we have chosen.

The inertial dissipation method was suggested as a means of flux estimation over the open ocean by Hicks and Dyer (1972) and developed and applied by Pond et al. (1979) and Large (1979). Based on the Kolmogorov hypothesis, the power spectral density $S_{uu}(n)$ of the downstream wind component u can, in the inertial subrange, be related to the dissipation rate ϵ via the wave number n:

$$S_{uu}(n) = K\epsilon^{2/3}n^{-5/3}, \quad (1)$$

where K is the one-dimensional Kolmogorov constant. This relationship assumes that the turbulence is isotropic, which may not be justified over the ocean [see

section 2c(3)]. Using Taylor's hypothesis, that is assuming "frozen" turbulence, Eq. (1) becomes

$$S_{uu}(f) = K\epsilon^{2/3} f^{-5/3} (U_{\text{rel}}/2\pi)^{2/3}, \quad (2)$$

where U_{rel} is the wind speed as measured by the anemometer and f is the measurement frequency. Hence, the dissipation rate can be obtained by calculating the mean value of $f^{5/3} S_{uu}(f)$ over an appropriate frequency range.

The wind stress is derived from the dissipation rate using the turbulent kinetic energy budget (e.g., see Busch 1972), which for steady-state horizontally homogeneous turbulence, can be written as

$$u_*^2 \frac{\partial \langle u' \rangle}{\partial z} + g \frac{\langle w' T_v' \rangle}{T_v} - \frac{\partial}{\partial z} \langle w' e' \rangle$$

$$P \quad + \quad B \quad - \quad D_t$$

$$+ \frac{1}{\rho} \frac{\partial}{\partial z} \langle w' p' \rangle = \epsilon \quad (3a)$$

$$+ \quad D_p \quad = \epsilon, \quad (3b)$$

where primes indicate fluctuations and angle brackets indicates mean quantities. In Eq. (3b) P is the mechanical production, B the buoyant production, and D_t and D_p are the vertical divergence of the turbulent transport and pressure transport terms; ϵ is the dissipation. Equation (3a) can be made dimensionless by multiplying by the Monin–Obukhov surface-layer scaling parameter kz/u_*^3 giving

$$\phi_m - \frac{z}{L} - \phi_t + \phi_p = \frac{\epsilon k z}{u_*^3} = \phi_\epsilon, \quad (4)$$

where the Obukhov length, L, is

$$L = \frac{-u_*^3 T_v}{(gk\langle T_v' w' \rangle_0)} \quad (5)$$

and each of the dimensionless profiles ϕ_m, ϕ_t, and ϕ_p are expected to be universal functions of z/L. Equation (4) defines the dimensionless dissipation function ϕ_ϵ. If the terms on the left-hand side of Eq. (4) are known [or equivalently the form of $\phi_\epsilon(z/L)$], the friction velocity can be evaluated from an estimate of the dissipation.

Unfortunately, the exact forms of $\phi_m(z/L)$, $\phi_t(z/L)$, and $\phi_p(z/L)$ are not well enough known (Fairall and Larsen 1986), and previous authors have made various assumptions as to their magnitude for turbulence over the sea. The form of $\phi_m(z/L)$ is critically dependent on the assumed value for the von Kármán constant k (Frenzen and Vogel 1994). Taking $k = 0.4$, Edson et al. (1991) reviewed several formulations for $\phi_m(z/L)$. The best performing formulas could be summarized by

$$\phi_m(z/L) = \begin{cases} [1 - \alpha(z/L)]^{-1/4}, & z/L < 0 \quad (6a) \\ 1 + \Gamma(z/L), & z/L > 0, \quad (6b) \end{cases}$$

where values of α ranging from 16 to 28 all fitted the data to a similar degree; Edson et al. (1991) chose a value $\alpha = 20$ because it gave the best overall fit with $\Gamma = 8$. However, Eqs. (6a)–(6b) still require further verification over the open ocean.

With regard to the vertical divergence terms, Large (1979) argued that the available evidence suggested that

$$\phi_t \approx -\phi_p. \quad (7)$$

This leads to a balance between dissipation and the sum of mechanical and buoyant production

$$\phi_\epsilon = \left(\phi_m - \frac{z}{L} \right). \quad (8a)$$

However, other authors, and the results presented in section 3, suggest that there is an imbalance between production and dissipation. Thus,

$$\phi_\epsilon = \left(\phi_m - \frac{z}{L} - \phi_D \right), \quad (8b)$$

where the imbalance term, $\phi_D = (\phi_t - \phi_p)$, is significantly larger than the uncertainty in the formula for ϕ_m.

As formulated above, the inertial dissipation technique requires assumptions with regard to the values of the von Kármán constant, the Kolmogorov constant K, and the form of the dimensionless functions $\phi_m(z/L)$ and $\phi_\epsilon(z/L)$. These constants and functions are not independent, and Fairall and Larsen (1986) have suggested a different formalization of the inertial dissipation method in terms of turbulence structure functions. As implemented by Edson et al. (1991), this requires determination of $\phi_m(z/L)$ and the dimensionless structure function parameter $f_u(z/L)$ but does not require an explicit Kolmogorov constant value. Whichever formalization is used, the number of assumptions and uncertainties are such that the best policy would seem to be to choose a consistent set of definitions that has been confirmed by comparison between eddy correlation and inertial dissipation results. Since the work of Large (1979) and Large and Pond (1981, 1982) represents the main verification of the inertial dissipation method over the open ocean, the analysis for this paper has been largely based on their formulation (section 2c). As in Large (1979), our analysis initially assumes a balance between production and dissipation (section 3a), but an imbalance term is found to be necessary and is formulated in section 3b and used thereafter.

b. Instrumentation and data recording

1) *Discovery* Southern Ocean cruises

The RRS *Discovery* Southern Ocean cruises took place between the end of December 1992 and the start of May 1993; the ship's track is shown in Fig. 1. A Solent Sonic Research Anemometer (manufactured by

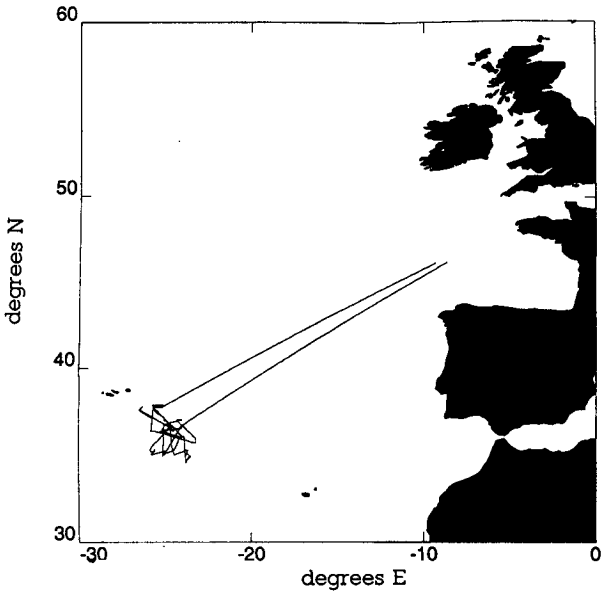

FIG. 2. SOFIA *Le Suroit* track plot.

Gill Instruments Ltd.) was mounted on the foremast 18.5 m above the sea surface. The asymmetric head version of the anemometer was used with the 240° open sector facing the bow of the ship. The anemometer provided digital three-component wind estimates at 21 Hz based on an acoustic sampling rate of 168 Hz. These data were sampled using a NEC APC IV portable microcomputer for four 12-min sampling runs each hour. The wind speed was calculated using all three components from the sonic anemometer and horizontal wind speed spectra were computed for 15 sections of 1024 samples. The steps in the spectral processing were (i) subtract the mean value for each section, (ii) apply a partial cosine window to the data, (iii) calculate the spectrum using a fast Fourier transform, (iv) correct for windowing loss and convert to spectral density, and (v) average the 15 spectra. To avoid contamination by ship motions, the mean value of $f^{5/3}S(f)$ was calculated over the 2 to 4 Hz frequency range and a linear fit calculated over the same range. The data stored for each run included the slope and intercept of this fit (used to quality control the data), the mean spectral level, and the mean wind speed U_{rel} during the 12-min run.

To enable the stability to be estimated, two Vector Instrument aspirated psychrometers (mounted near the sonic anemometer), an aneroid barometer, and a hull-mounted platinum resistance thermometer (for sea temperature) were used to record average values at 1-min intervals. The analogue channels of the Solent Sonic were also sampled by the mean meteorological logger. One-minute mean data on the ship's speed both over ground and through the water were produced from the ship's Global Positioning System (GPS) system and a two component electromagnetic log system, respectively.

2) *Le Suroit* SOFIA cruises

For the SOFIA experiment (May–June 1992) in the Azores region (Fig. 2), an asymmetric Solent Sonic anemometer was mounted 16 m above sea level on a 10-m meteorological mast on the bow of *le Suroit.* The sonic anemometer logging and spectral computation were as described for *Discovery.* The mean meteorological data were logged on an IOSDL MultiMet system (Birch and Pascal 1987), which recorded 1-min samples based on 1-Hz sampling over a 50-s period. Sensors were similar to those used on *Discovery* except that a trailing thermistor was used to measure sea surface temperature. A GPS and compass system was used to record the ship's speed over the ground. The fore and aft component of the ship's speed through the water was available from an electromagnetic log. Initial results from the SOFIA experiment have been reported by Dupuis et al. (1995).

c. *Data analysis method*

1) Quality control procedures

During the postcruise data analysis, averages of the mean meteorological and navigation data were calculated to correspond to the time periods of the sonic anemometer sampling runs. Quality control criteria were applied to the data and a run was rejected if: the slope of the wind speed spectra was not within 30% of a (frequency)$^{5/3}$ relationship: the wind was not blowing within 30 deg of the bows; the standard deviation of the 1-min values for either the relative wind direction or the ship's head was greater than 20 deg; or the standard deviation in the ships speed was greater than 0.5 m s^{-1}. The latter two criteria were designed to reject runs during periods when the ship was maneuvering. The amount of data remaining after this selection process is summarized in Table 1 [section 4b(2)].

2) Calculation of friction velocity

The wind stress was calculated following the inertial dissipation method formulation described in section 2a. The dissipation rate was determined from the recorded values of the mean spectral level using Eq. (2) and the friction velocity calculated from Eq. (4) with the stability function $\phi_m(z/L)$ given by Eq. (6). Using a von Kármán constant, $k = 0.4$, and following Edson et al. (1991), $\alpha = 20$ was used in Eq. (6a). However, $\Gamma = 5$ was used in Eq. (6b) in order that $\partial\phi_m/\partial(z/L)$ should be continuous across $z/L = 0$.

3) Choice of the Kolmogorov constant

For this paper, $K = 0.55$ has been used. This follows Large and Pond (1981), who assumed 0.55 to be the

TABLE 1. Drag coefficient relationship (obtained by one-way regression).

Study	$1000C_{D10n}$ =	r	U_{10n} (m s^{-1})	Data	Anemometer
This study	$0.60 + 0.070U_{10n}$	0.74	6–26	2298	
	$0.29 + 3.1/U_{10n} + 7.7/U_{10n}^2$		0–6	166	Solent Sonic
Large and Pond (1981/82)	$0.49 + 0.065U_{10n}$	0.74	10–26	973	
	1.14		4–10	618	K Gill propeller
Smith (1980)	$0.61 + 0.063U_{10n}$	0.70	6–22	63	thrust
Anderson (1992)	$0.49 + 0.071U_{10n}$	0.91	4.5–18	84	
	$0.59 + 0.065U_{10n}$	0.83	10–18	61	Gill propeller
Geernaert et al. (1988)	$5/U_{10n} + 0.07U_{10n}$		3–10	130	sonic and hot film

value of the Kolmogorov constant and found good agreement between eddy correlation and inertial dissipation wind stress measurements. Similarly, the eddy correlation and inertial dissipation comparisons of Edson et al. (1991) implied that $K = 0.55$. However, the latter authors suggested that this represents an effective Kolmogorov constant K_{eff} and that the true value was approximately 0.51. Deacon (1988) defined K_{eff} as the value required to calculate the correct value of u_* [from Eq. (4)] assuming that production balances dissipation [Eq. (8a)]. He reviewed previous estimates of K_{eff} and for the measurements over water (mainly for winds < 10 m s^{-1}) found a range for K_{eff} from 0.50 to 0.77 with a mean of 0.60. If $K_{\text{eff}} > K$, then the use of K_{eff} may be viewed as compensating for an excess of dissipation over production at neutral stability. Assuming that a further imbalance term, ϕ'_D, is required at nonneutral stabilities, it can easily be shown from Eqs. (2) and (4) that the use of K_{eff} implies a total imbalance term in Eq. (8b) of

$$\phi_D = (1 - \gamma)\left(\phi_m - \frac{z}{L}\right) - \gamma\phi'_D, \qquad (9)$$

where

$$\gamma = \left(\frac{K_{\text{eff}}}{K}\right)^{3/2}.$$

For example, if $K_{\text{eff}} = 0.55$ and $K = 0.52$, then at neutral stability Eq. (9) implies an imbalance of about 10%.

A possible inconsistency in the use of the dissipation method must also be noted here. The spectral values calculated were for the wind speed rather than the downstream component required for Eq. (1). We originally chose to do this in an attempt to simulate the method used by Large and Pond (1981, 1982), who applied the dissipation formulas to the wind speed as measured by the propeller–vane anemometer. However, during our development of the system we also computed a few spectral values using the downstream component and obtained essentially the same spectral level. This suggests that the ratio of the cross-stream to alongstream spectra is close to 1 rather than the $4/3$ value expected if the turbulence were isotropic. Schmitt et al. (1978) report a similar finding. Reviewing the ratio of vertical to streamwise spectral levels published by previous authors they found that, in contrast to results for turbulence over land, the ratio over the sea averaged 1.06 ± 0.16. This apparent anisotropy questions the basis of Eq. (1) for measurements over the sea. However, the comparisons with the eddy correlation method (for example, Edson et al. 1991; Large and Pond 1981) suggest that the inertial dissipation method does work. Possibly the effects of anisotropy have been compensated by the use of an effective value for the Kolmogorov constant.

4) CALCULATION OF THE STABILITY PARAMETER (z/L)

To calculate the Obukhov length, the virtual temperature scale, T_{v*}, was estimated from bulk formula calculations of the temperature and humidity scaling parameters, T_* and q_*. Since the transfer coefficients are conventionally defined for 10-m height and neutral stability, the calculations would be considerably simplified by first evaluating the 10-m neutral values for all quantities. However, it was found that the iterative method used failed to converge on a few occasions, so following Large (1979), the evaluations have been performed using the observed height and stabilities. Thus,

$$T_* = C_T u_z(\theta_a - T_s)/u_* \qquad (10a)$$

$$q_* = C_q u_z(q_a - q_s)/u_*, \qquad (10b)$$

where the potential air temperature, $\theta_a = T_a + 0.00976z_T$, where z_T is the height in meters at which the air temperature T_a and humidity q_a were measured. The sea surface humidity q_s was calculated assuming 98% saturation at the sea surface temperature T_s. The 10-m neutral transfer coefficients used were those of Smith (1988), who suggests ($C_{T10n} = 1.0 \times 10^{-3}$, $C_{q10n} = 1.2 \times 10^{-3}$), adjusted for height and stability following Large (1979). For example,

$$C_T = \frac{C_{T10n}\left(\frac{C_D}{C_{DN}}\right)^{1/2}}{1 + \left(\frac{C_{T10n}}{kC_{D10n}^{1/2}}\right)\left[\ln\left(\frac{z_T}{10}\right) - \Psi_t\right]}, \quad (11)$$

and similarly for C_q, where

$$C_D = C_{D10n}\left\{1 + \frac{(C_{D10n})^{1/2}}{k}\left[\ln\left(\frac{z_u}{10}\right) - \Psi_m\right]\right\}^{-2}. \quad (12)$$

The neutral value of the drag coefficient was calculated iteratively along with u_*:

$$C_{D10n} = u_*^2/U_{10n}^2 \quad (13)$$

[see subsections (5) and (6)]. Finally, the virtual temperature scale was calculated from (e.g., Stull 1988, appendix D)

$$T_{v*} = T_* + 0.61T_{10n}q_*, \quad (14)$$

and hence the stability parameter

$$\frac{z}{L} = \frac{z(gkT_{v*})}{(T_{v10n}u_*^2)}. \quad (15)$$

5) REDUCTION TO 10-M NEUTRAL VALUES

Calculation of 10-m neutral values was performed using the standard profile formulas

$$u_z = u_0 + \frac{u_*}{k}\left[\ln\left(\frac{z_u}{z_0}\right) - \Psi_m\right] \quad (16a)$$

$$T_z = T_0 + \frac{T_*}{k}\left[\ln\left(\frac{z_t}{z_0}\right) - \Psi_t\right], \quad (16b)$$

where q_z behaves similarly to T_z; u_0, T_0, and q_0 are the surface values. The stratification functions Ψ_i were as defined by Paulson (1970); for momentum,

$$\Psi_m = \begin{cases} 2\ln\left(\frac{1+\phi_m^{-1}}{2}\right) + \ln\left(\frac{1+\phi_m^{-2}}{2}\right) & (17a) \\ \quad - 2\tan^{-1}\phi_m^{-1} + \frac{\pi}{2}, \quad (z/L < 0) & \\ 1 - \phi_m, \quad (z/L > 0), & (17b) \end{cases}$$

and for temperature and humidity,

$$\Psi_t = \Psi_q = 2\ln\left(\frac{1+\phi_m^{-2}}{2}\right) \quad (z/L < 0) \quad (18a)$$

$$\Psi_t = \Psi_q = 1 - \phi_m \quad (z/L > 0). \quad (18b)$$

6) CALCULATION OF THE TRUE WIND SPEED AND THE DRAG COEFFICIENT

Calculation of the friction velocity u_* only requires knowledge of the relative wind at the anemometer [U_{rel} in Eq. (2)]. However, calculation of the drag coefficient C_{D10n} requires knowledge of the true wind speed U_{10n} derived from the relative wind and the ship's velocity. The ship's velocity with respect to the ground, as determined by the ship's GPS satellite navigation system, was used for this purpose. This follows the precedent of previous papers in neglecting the effects of any ocean current, whether locally wind driven or due to large-scale ocean circulations. Using data from the North Sea, Geernaert et al. (1986) and Smith et al. (1992) explicitly made allowance for the effect of the strong tidal currents on their wind stress estimates. Other authors have assumed that the effects of mean ocean currents are negligible. Thus, the effect of any wind drift current due to the local wind and waves has effectively been parameterized into the drag coefficient determinations.

An estimate of the ocean currents, and hence the error introduced by referencing the ship's velocity relative to the ground, should be obtained by comparing the ship's speed over the ground from the GPS to the ship's speed through the water from the electromagnetic log data. Unfortunately, it is difficult to obtain an accurate calibration of the em log, particularly at the low ship speeds characteristic of research vessels. Thus, our initial estimates of the ocean currents were of order a few tenths meters per second and of a nature that, particularly in the case of the SOFIA data, suggested em-log calibration errors. To calibrate the em-log the assumption has to be made that for each dataset as a whole the component of the (nonwind induced) ocean current in the wind direction was not significant in the mean. This seems valid given the large areas traversed by the cruises (Figs. 1 and 2) and the variation of wind direction during a cruise. However, it is likely that there would have been a nonzero mean component of the wind-induced drift current along the wind direction. This has been estimated by calibrating the fore and aft component of the em-log against the GPS system as a function of ship speed (noting that the wind stress data were obtained with the wind on the bows). Only data for wind speeds below 12 m s^{-1} were used since a full range of ship speeds occurred in that wind speed range. The mean wind drift current was then estimated by calculating the mean difference between the fore and aft component of the GPS and em-log-deduced ship speeds as a function of wind speed. The resulting estimate of the wind drift is shown in Fig. 3. Both the *Discovery* and SOFIA data suggest negligible wind drift for wind speeds below 10 m s^{-1}. At higher wind speeds the *Discovery* data suggest that at the depth of the em-log (about 4 m) the mean wind drift magnitude is about 15% of the friction velocity. This implies that the error in calculating the wind speed due to referring the measurements to the solid earth was probably less than 0.2 m s^{-1} and not significant in the mean results presented below.

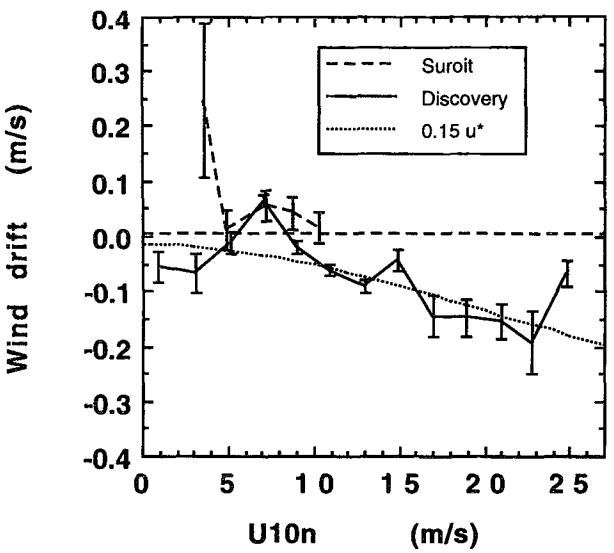

FIG. 3. Wind drift current (from GPS–em log ship speeds), against 10-m neutral wind speed for the *Discovery* cruises (solid line) and the SOFIA *Le Suroit* cruise (dashed). The dotted line indicates $0.15u_*$. Error bars show the standard deviation of the mean.

3. The nondimensional dissipation function

a. *Results assuming zero imbalance*

The *Discovery* Southern Ocean data were initially processed with the assumption of zero imbalance between dissipation and production [Eq. (8a), section 2a]. The resulting relationship between friction velocity and wind speed is shown in Figs. 4a and 4b for unstable and stable values respectively. The data have been separated into different stability ranges [represented for comparison purposes by the value of $[(10m)/L]$ and then the friction velocity averaged into 1 m s^{-1} U_{10n} bins. For clarity, only some of the stability ranges are shown, but the same trend applied throughout the range of stabilities encountered. It can be seen that the calculated friction velocity to wind speed relationship varied with the stability range selected; this should not be the case if the form of $\phi_m(z/L)$ and the assumption of zero imbalance are both correct. Figure 4a shows that, above 7 m s^{-1}, the friction velocity was increasingly underestimated for increasingly unstable data. This applied even in the range $-0.05 < 10/L < -0.01$, which has been considered "neutral" data in some studies. Similarly, Fig. 4b shows that below 7 m s^{-1} friction velocity was again underestimated for stable data. The apparent dependence of the u_* to U_{10n} relationship on stability was much greater than could be accounted for by any of the accepted variations in the formula for $\phi_m(z/L)$ reviewed by Edson et al. (1991); the assumption of zero imbalance must therefore be false.

b. *Determination of the imbalance term*

If the form of the imbalance term was correct, then for a given wind speed there should be no dependence of the friction velocity on $10/L$. In order to formulate such a term from the *Discovery* data, it was assumed that there was a balance between production and dissipation under neutral conditions. The form of the imbalance under nonneutral conditions was then determined in relation to the neutral data. The validity of this assumption and the implications of a possible imbalance under neutral conditions are both discussed in section 3c.

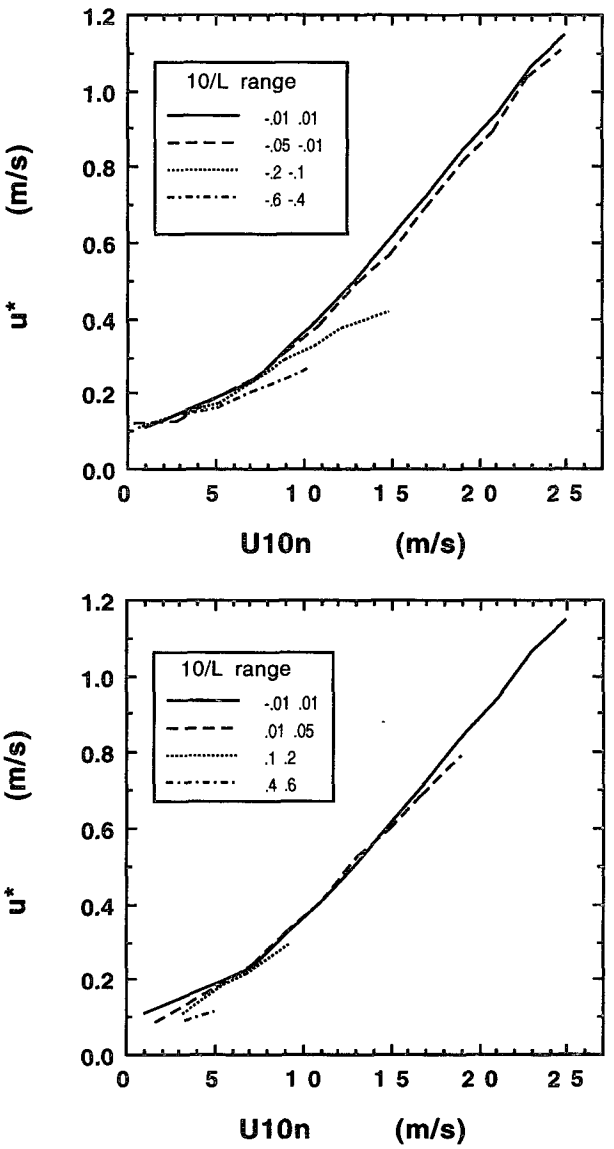

FIG. 4. Friction velocity, calculated assuming zero imbalance, against U_{10n} for *Discovery* data obtained under (a: top) unstable and (b: bottom) stable conditions. To avoid confusion, only some of the stability ranges are shown.

The form of the imbalance term was determined for the nonneutral data by comparison with neutral data. A friction velocity to U_{10n} relationship was obtained for neutral conditions using data where $|10/L| < 0.005$. This relationship was used in the bulk formula and applied to the air and sea temperatures and mean wind data to calculate the friction velocity and stability parameter for the entire dataset. The form of the implied dimensionless dissipation function ϕ_ϵ was then calculated using Eq. (4); it is shown in Fig. 5a as a function of $10/L$. The data are separated into different wind speed ranges and a solid line illustrating Eq. (8a) (zero imbalance) is also shown.

Figure 5a shows that the assumption of zero imbalance may be reasonable at low winds (3–7 m s^{-1}) but not at moderate to high wind speeds in unstable conditions. For these conditions the different wind speed ranges need different forms of ϕ_ϵ, with an imbalance term that increases as U_{10n} increases from moderate to high winds. For stable conditions there is insufficient data at moderate and high wind speeds to clearly define the wind speed dependence. However, Fig. 4b implies that an imbalance term is needed to increase the u_* values for stable conditions, particularly below 7 m s^{-1}. After some experimentation, imbalance terms of the form

$$\phi_D = \begin{cases} \dfrac{z}{L}\left(2 - \dfrac{U_{10n}}{3}\right), & z/L \leq 0 \quad (19a) \\ \dfrac{z}{L}\left(\dfrac{(U_{10n} - 12)^2}{15}\right), & z/L > 0, \quad (19b) \end{cases}$$

although not truly nondimensional, were found to produce the best agreement between neutral and nonneutral data. The implications of a wind-speed-dependent imbalance term are discussed in section 3c. Figure 5b shows the form of ϕ_ϵ when these imbalance terms are included in the dissipation function [Eq. (8b)]. It may be compared with the observed ϕ_ϵ shown in Fig. 5a. For unstable data the resulting ϕ_ϵ values are clearly similar to the observations. For stable conditions the agreement does not appear as good. The effect of this imbalance term on the friction velocity to U_{10n} relationship is shown in Figs. 6a and 6b for unstable and stable data respectively. Except for the extremes of the wind speed range, the unstable data now overlie the neutral data. For stable data (Fig. 6b), there is an improvement at low and moderate wind speeds. It is this improvement that justifies the suggested form of Eq. (19b); however, it must be stated that, whereas Eq. (19a) is well defined by the data from unstable conditions, the stable form (19b) is much less well defined.

To produce Figs. 6a,b, the data were assigned to stability ranges using the $10/L$ value produced by the original processing, rather than that which resulted from the analysis that included the imbalance term. This allows direct comparison between Figs. 4 and 6 and illustrates how the friction velocity to U_{10n} relationship has improved. However, inclusion of the imbalance term significantly affected the calculation of $10/L$, as shown in Fig. 7a. The $10/L$ values were generally reduced toward the neutral value, particularly for stable conditions. The resulting distribution of stability against wind speed is shown in Fig. 7b. It must be emphasized that the forms of the imbalance terms sug-

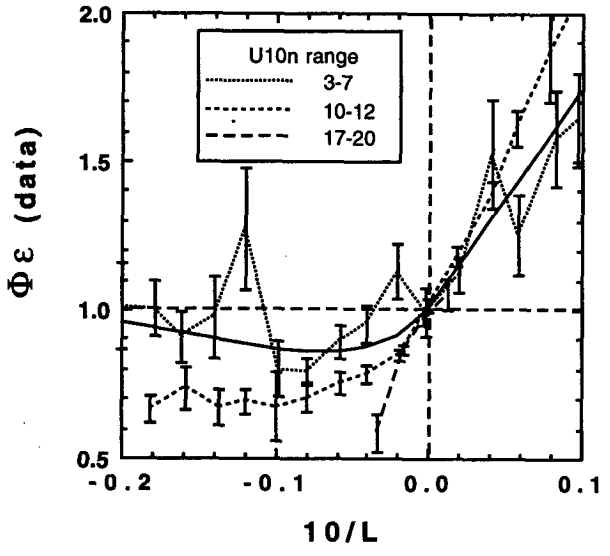

FIG. 5. (a) Implied dimensionless dissipation function calculated from *Discovery* data for three different wind speed ranges. Error bars indicate standard deviation of the mean. The continuous line represents the balance between production and dissipation.

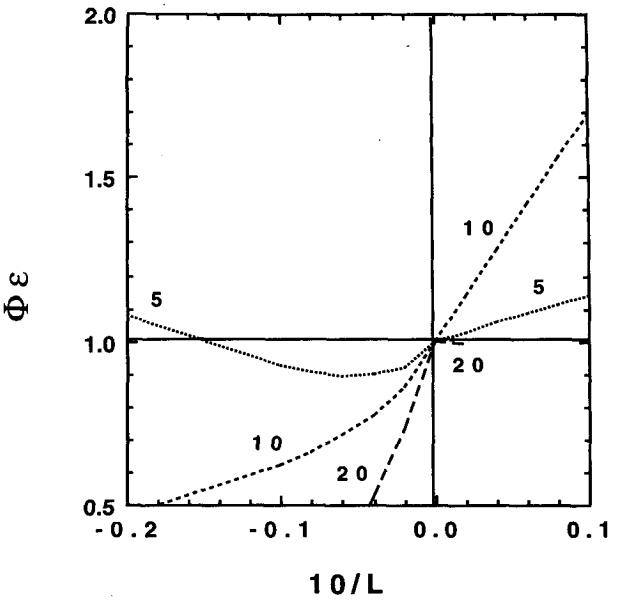

FIG. 5. (b) Dimensionless dissipation function, including imbalance terms from Eqs. (19a) and (19b), calculated for wind speeds of 5, 10, and 20 m s^{-1}.

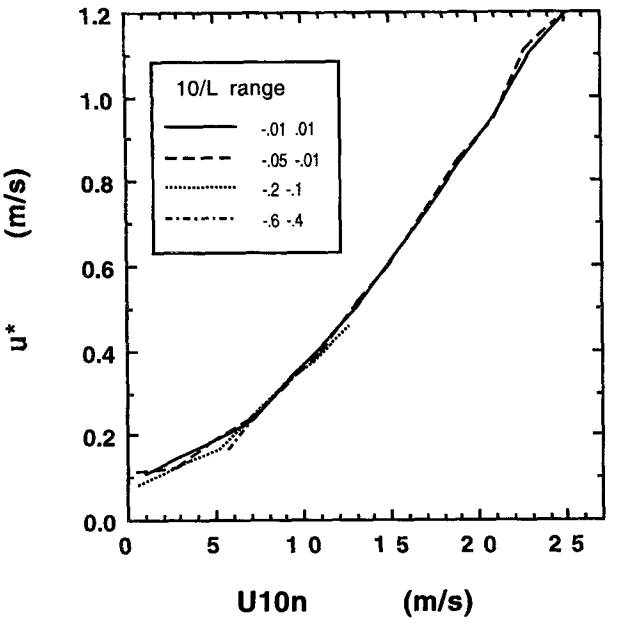

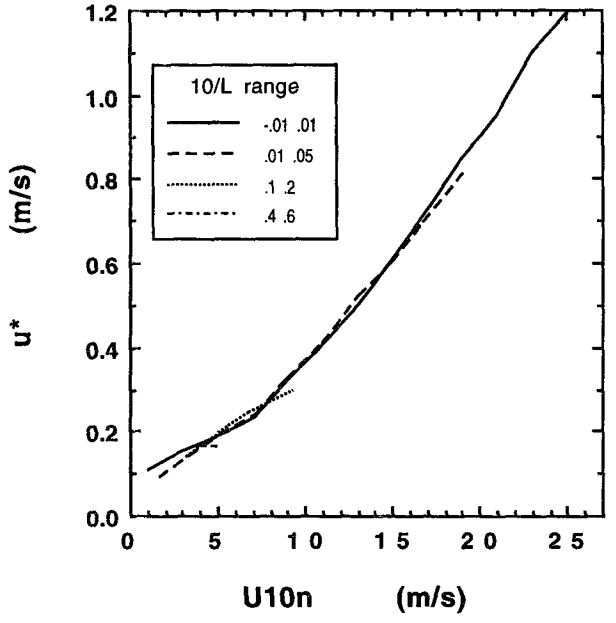

FIG. 6. Friction velocity, calculated assuming imbalance terms [Eqs. (19a) and (19b)], for *Discovery* data obtained under (a: top) unstable and (b: bottom) stable conditions. Data are grouped by stability ranges exactly equivalent to those in Fig. 4.

gested in Eq. (19) are only established over the combined stability and wind speed ranges shown in Fig. 7b.

c. Discussion

Figure 8a shows the form of the wind-speed-dependent imbalance terms [Eqs. (19a)–(19b)] as a function of stability for three different wind speeds. At each

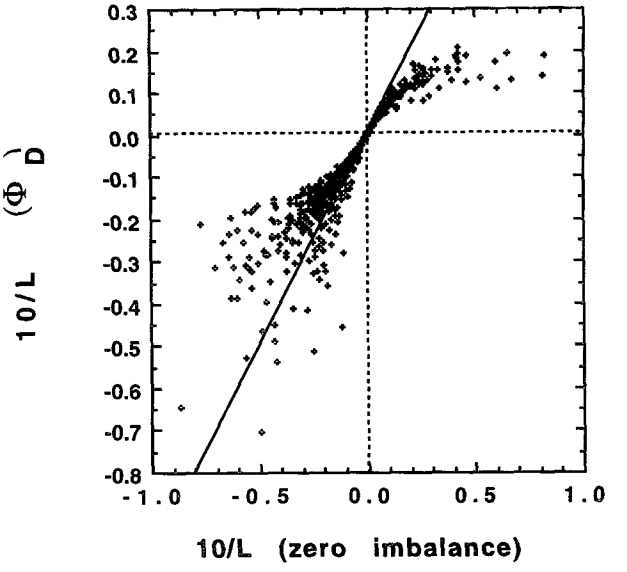

FIG. 7. (a) Stability parameter calculated with and without imbalance terms. Solid line indicates 1:1 agreement.

wind speed, ϕ_D has only been plotted for the range of stability encountered. That the required imbalance term varied with wind speed as well as stability is not implausible over the ocean where the surface roughness elements may also vary with wind speed. For most wind speeds and stabilities, even a very small departure from neutral stability resulted in a rapid increase of ϕ_D. Thus, Fig. 8a predicts a significant stability-dependent correction for inertial dissipation data that other studies may have treated as taken under neutral conditions.

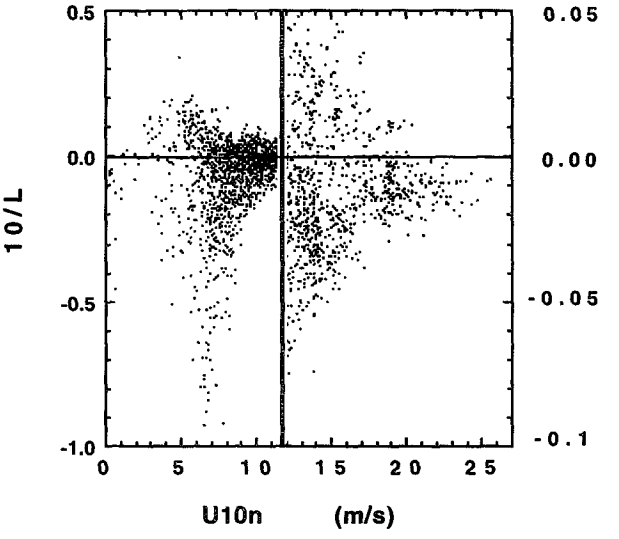

FIG. 7. (b) Distribution of stability parameter 10/*L* (calculated with imbalance terms) against 10-m neutral wind speed. Note change of scale at 12 m s^{-1}.

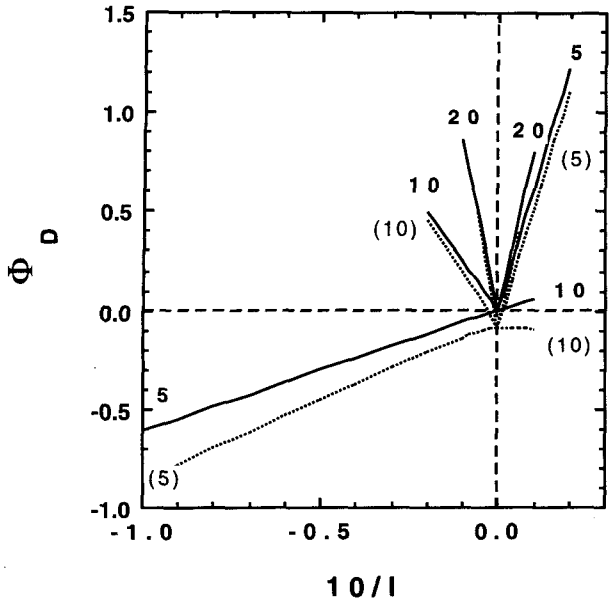

FIG. 8. (a) Form of the imbalance term ϕ_D as a function of $10/L$, shown for wind speeds of 5, 10, and 20 m s^{-1} and for Kolmogorov constants of 0.55 (solid line) and 0.52 (dotted line). The term is positive when production exceeds dissipation.

Interpretation of these functions in terms of the balance between production and dissipation of turbulent kinetic energy depends on knowledge of the true value for the Kolmogorov constant. If the value used (0.55) represents the true value, then Fig. 8a shows that for most conditions ϕ_D is positive, implying that local production exceeds dissipation. Here ϕ_D is negative (dissipation exceeds local production), only when unstable conditions combine with low wind speeds ($U_{10n} < 6$ m s^{-1}). The observed values of ϕ_D for the Southern Ocean data are shown in Fig. 8b as a function of wind speed. At any given wind speed (above ~10 m s^{-1}) the ϕ_D values range from 0 (those at neutral stability) to about +0.2 (for the most stable or unstable values). Except at low wind speeds the mean ϕ_D value, averaged over all observed stabilities, is about 0.1, implying an excess of local production over dissipation of 10%.

However, if the true value of the Kolmogorov constant is 0.52 (e.g., see Frenzen and Vogel 1992), then our value of 0.55 is an effective Kolmogorov constant. As discussed in section 2c(3), this implies that there is an imbalance even at neutral stability. The total imbalance term that would then be calculated [from Eq. (9)] is also shown in Fig. 8a. As expected, the major changes occur in very close to neutral conditions where the implication is that dissipation exceeds local production, rather than the previous assumption of balance. Dissipation is also found to exceed local production at about 10 m s^{-1} under stable conditions. In Fig. 8b the effect would be to decrease the ϕ_D values by about 0.1 with, on average, near balance between production and dissipation. However, it must be stressed that this is an average value only; the stability and wind-dependent variation of ϕ_D still remains, and it would not be correct to assume $K = 0.52$ and $\phi_D = 0$, even for neutral stability.

Figure 8a shows that, for most stability values, ϕ_D (and hence the balance between dissipation and production) reverses sign in the wind speed range typical of previous studies, 3 to 10 m s^{-1}. Thus, comparison of our results with other authors critically depends both on the assumed Kolmogorov constant and on the range of wind speeds and stabilities encountered, details which are not always available. Most previous authors have assumed that $K = 0.52$ in which case, for unstable data, we find that dissipation is greater than production by up to 10% if $|10/L| < 0.1$ and/or the wind speed is less than 9 m s^{-1}. For more unstable data and greater wind speeds we find that production exceeds dissipation. Schacher et al. (1981) found a balance between production and dissipation for unstable data and wind speeds of about 3–8 m s^{-1}, where we would also predict a balance (Fig. 5a). For stable conditions they were more in agreement with the land-based results of Wyngaard and Coté (1971), which suggested that dissipation exceeded local production. Other studies have reached conflicting conclusions. Edson et al. (1991) suggested that reinterpretation of the Wyngaard and Coté (1971) results, using the more commonly accepted value of the von Kármán constant,

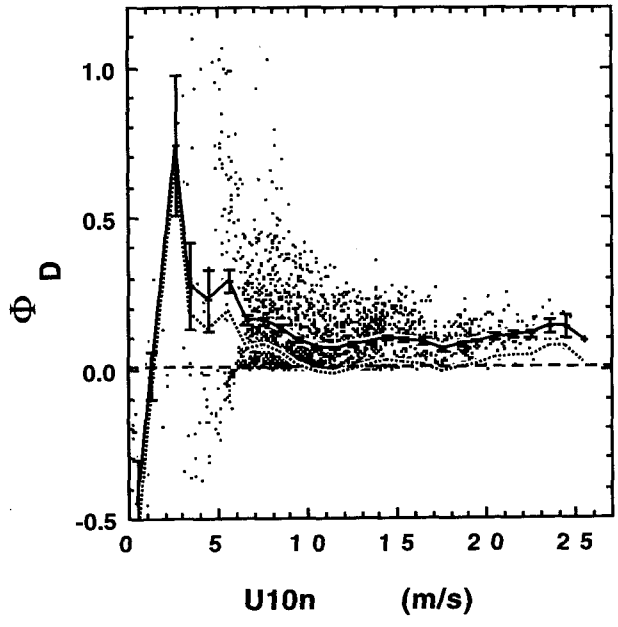

FIG. 8. (b) Distribution of ϕ_D values against wind speed for the *Discovery* data. The solid line indicates the mean value and the error bars indicate the standard deviation of the mean. The dotted line indicates the mean value if a Kolmogorov constant of 0.52 were to be used instead of 0.55.

$k = 0.4$, was consistent with their HEXMAX result of an excess of dissipation over production of about 12%. However, Fairall and Edson (1994) analyzed the HEXMAX data along with data from RV *FLIP* and RV *Iselin* and found that local production exceeded dissipation by about 10%. Frenzen and Vogel's (1992) dissipation measurements also suggested that dissipation is less than production, by about 20%. They too reinterpreted the data of Wyngaard and Coté (1971) and found that dissipation was about 16% less than production. The contradictions between these various formulations may be explained, at least in part, if the imbalance term does indeed depend on both stability and wind speed, as our results suggest.

Ideally, the ϕ_D formulas of Eqs. (19a)–(19b) should be expressed in a properly dimensionless form. The wind speed dependence may, in fact, be due to sea state and hence roughness Reynolds number. In that respect, it is noteworthy that under unstable conditions [Eq. (19a)] ϕ_D changes sign at about the wind speed at which the airflow is thought to become fully turbulent (e.g., Wu 1980). At lower wind speeds, the flow may enter a "transitional" stage between turbulent and laminar flow. Since the imbalance term for stable conditions is based mainly on low wind speed data, Eq. (19b) is very tentative. These problems do not apply to the imbalance term for the unstable case (19a) since it is derived from a large number of data across the entire range of wind speeds.

To properly verify our assumption of a wind-speed-dependent imbalance term would require a comprehensive study of the turbulent kinetic energy budget over the ocean similar to that described by Frenzen and Vogel (1992) for an inland site. Unfortunately, the experimental difficulties posed by an open ocean site, and the range of stability and wind speed conditions necessary, would render such studies extremely difficult to perform. An alternative, less direct method is to compare concurrent eddy correlation and dissipation data. Existing studies are generally restricted either to low wind speed conditions in the open ocean (Fairall and Edson 1994) or to a coastal platform (Edson et al. 1991), which may not be representative of open ocean conditions. The results have not been presented in terms of varying wind speed. Again, obtaining suitable open ocean data under a wide range of conditions would pose severe experimental problems.

4. Wind stress, drag coefficient, and wind speed relationships

a. Drag coefficient to wind speed relationship

The relationship between the mean friction velocity and drag coefficient and the 10-m neutral wind speed has been calculated from the *Discovery* Southern Ocean data using the wind-dependent imbalance term described in section 3b. The number of data in each 1-m s^{-1} wind speed range are shown in Fig. 9. Below 3 m s^{-1} and above 23 m s^{-1} there are less than 10 values in each 1-m s^{-1} average; the majority of the data lie in the range of 5–20 m s^{-1} where there are more than 50 data in each average. For our measurement height of 18.5 m, this implies a wind speed precision of better than 0.5% for winds of 3 m s^{-1} or greater (Wyngaard 1973).

Figure 10a shows the mean relationship of C_{D10n} to U_{10n}, where the data have been averaged into 1 m s^{-1} wind speed ranges; error bars indicate the standard error of the mean. The mean relationship for neutral data ($|10/L| < 0.01$) was indistinguishable from the one shown. The dashed line shows the one-way regression for all data above 6 m s^{-1}, represented by

$$1000C_{D10n} = 0.60 + 0.070U_{10n}, \quad (6 \leq U_{10n} \leq 26 \text{ m s}^{-1}). \quad (20a)$$

The regression coefficient was 0.74, the standard error of the slope was ±0.001 and the standard error of the intercept was ±0.02.

At lower wind speeds, below 6 m s^{-1} (Fig. 10b) the data may be represented by the relationship

$$1000C_{D10n} = 0.29 + \frac{3.1}{U_{10n}} + \frac{7.7}{U_{10n}^2}, \quad (U_{10n} \leq 6 \text{ m s}^{-1}). \quad (20b)$$

Also shown in this figure are the low wind speed results from *le Suroit*, which lie within the scatter of the *Discovery* data but fall slightly below the mean relationship.

An alternative representation of the results is to examine the variation of the friction velocity u_* with U_{10n}; individual data values are shown in Fig. 11a. Also shown are the friction velocity values implied by the

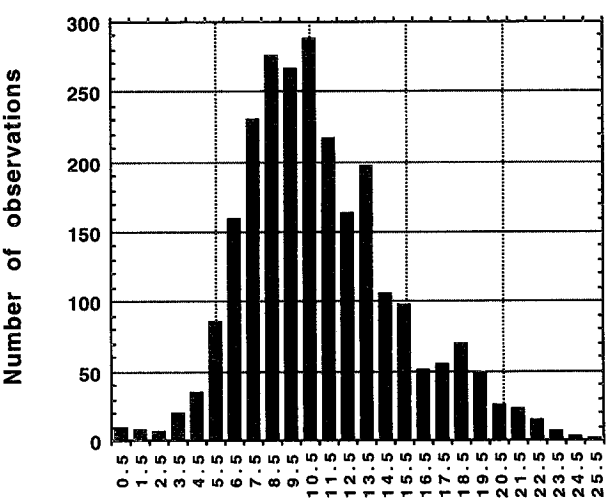

FIG. 9. Histogram showing number of data per 1 m s^{-1} of the 10-m neutral wind speed.

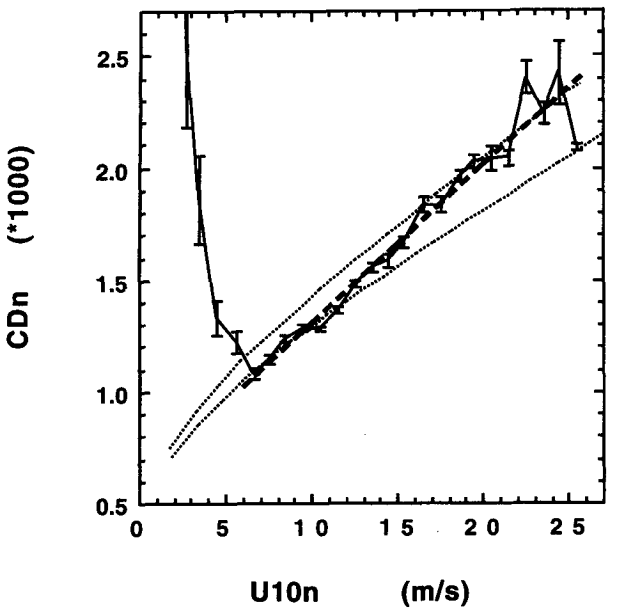

FIG. 10. (a) Drag coefficient results from the *Discovery* data for wind speeds above 6 m s^{-1}. Error bars indicate standard deviation of the mean. The C_{D10n} to U_{10n} relationship of Eq. (20a) is shown by the dashed line. Also shown are Charnock relationships with constants of 0.011 (lower dotted) and 0.017 (upper dotted).

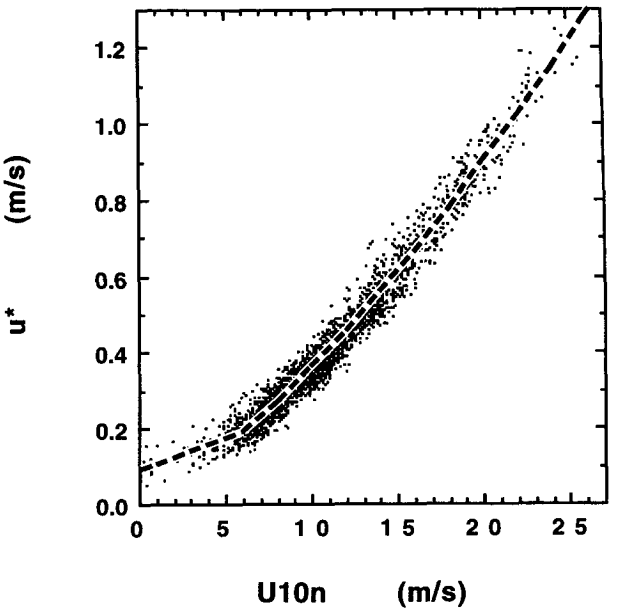

FIG. 11. (a) Individual friction velocity data from the *Discovery*. The dashed line shows the friction velocity values implied by the C_{D10n} to U_{10n} relationships of Eq. (20a) and Eq. (20b).

C_{D10n} to U_{10n} relationships. It can be seen that these represent the data very well across the entire range of wind speeds, especially above 6 m s^{-1}. Indeed it must be stressed that in the higher wind speed range a linear C_{D10n} to U_{10n} relationship [Eq. (20a)] was chosen, not for convenience but because it was an excellent fit to the observed data. The low wind speed values (Fig. 11b) from both *Discovery* and SOFIA show the change in the relationships occurring at about 6 m s^{-1}.

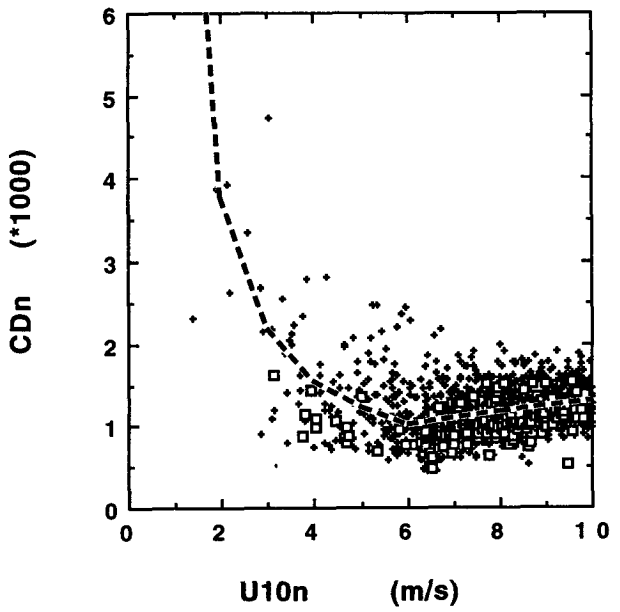

FIG. 10. (b) As Fig. 10a but individual low wind speed data points from the *Discovery* (crosses), and *Le Suroit* (squares). The dashed line indicates the relationship of Eq. (20b).

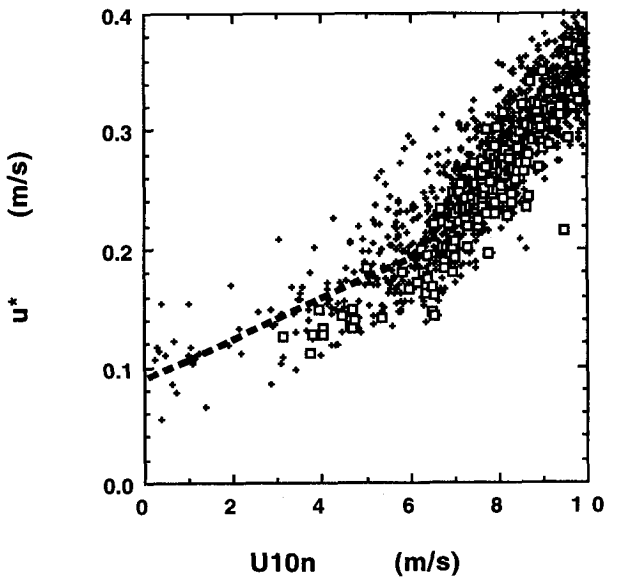

FIG. 11. (b) As in Fig. 11a but showing individual friction velocity results from the *Discovery* (crosses) and *Le Suroit* (squares) for low wind speed data.

Using the data in Fig. 11a, it is possible to fit a polynomial to the friction velocities over all wind speeds

$$u_* = 0.10038 + 0.00217U_{10n} + 0.00278U_{10n}^2 - 0.000044U_{10n}^3. \quad (21)$$

This, though cumbersome, avoids the discontinuity at 6 m s^{-1} and is a very good fit to the data ($r = 0.98$). However, this friction velocity relationship has the disadvantage that it must not be extrapolated above 26 m s^{-1}. It would predict decreasing wind stress values for wind speeds above 30 m s^{-1}, which have no basis either in our data or in the review of Garratt (1977).

b. *Discussion*

1) Low wind speeds

The C_{D10n} to U_{10n} relationships [Eq. (20)] are compared in Fig. 12 to relationships proposed in previous studies. We consider first the results at wind speeds below 6 m s^{-1}. Although each of the data points shown in Figs. 10b and 11b have passed the various quality control criteria [section 2c(1)], it might reasonably be questioned whether the assumptions implicit in the inertial dissipation method hold true at these low wind speeds. However, comparison can be made with data obtained using the eddy correlation technique under low wind speed conditions off the Californian coast that have been published by Geernaert et al. (1988). These data, shown in Fig. 12b, are similar to our results and are well fitted by the C_{D10n} to U_{10n} relationship proposed here [Eq. (20b)], thus providing some reassurance with regard to the inertial dissipation results.

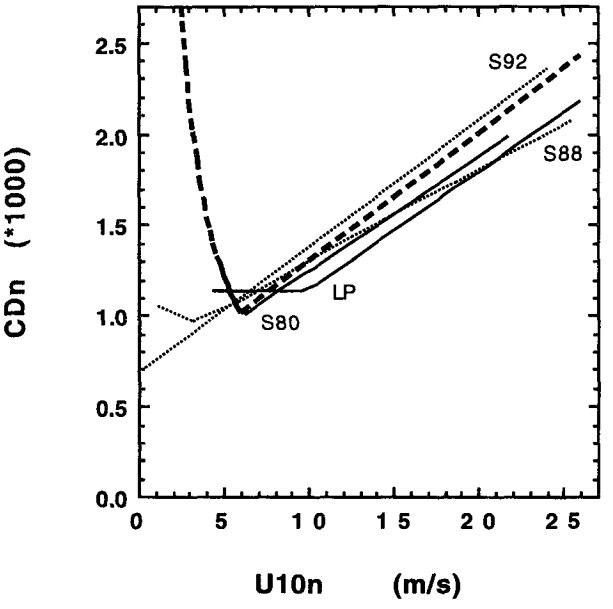

FIG. 12. (a) Comparison of drag coefficient relationships: results from this study (dashed line), Smith et al. 1992 (upper dotted), Smith 1980 (upper solid), Large and Pond 1981/82 (lower solid), and Smith 1988 (lower dotted).

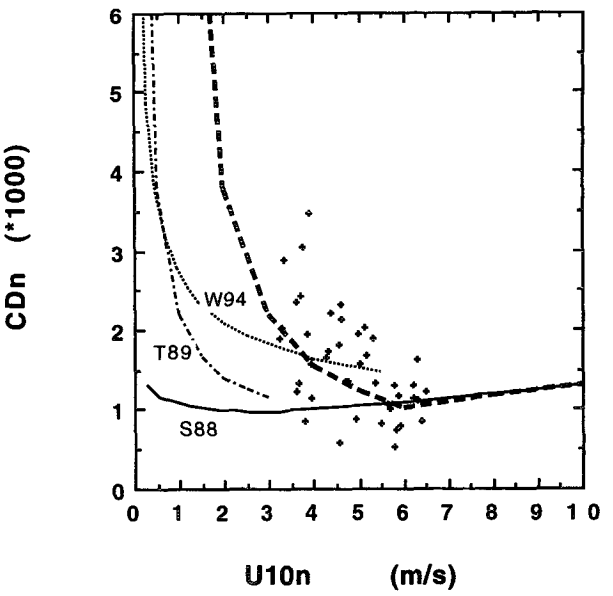

FIG. 12. (b) Eddy correlation data from Geernaert et al. 1988 (crosses), and low wind speed drag coefficient relationships: Equation (20b) from this study (dashed line), Wu 1994 (dotted), Trenberth et al. 1989 (chain), and Smith 1988 (solid).

On the other hand, it seems very unlikely that, at zero wind speed, the friction velocity should take a value of 0.1 m s^{-1} as our low wind speed formulas [Eqs. (20b) and (21)] imply. Geernaert and Plant (1990) suggest, as a working formula for the height H_s of the surface layer, $H_s = AU_{10n}$ (where A is about 10 s). Thus, about 2 m s^{-1} would represent the lowest wind speed for which the *Discovery* measurements would have been within the surface layer under neutral conditions. Although this wind speed limit would be higher in stable conditions, and lower in the unstable conditions for which most of the low wind speed data were obtained, we should assume that for data below, say 3 m s^{-1}, the measurements were not definitely within the surface layer. In that case, scaling with u_* is no longer appropriate and measurements at a lower height are required. The few *Discovery* data below 3 m s^{-1} were in any case very scattered (Fig. 10b) and the C_{D10n} poorly defined.

Considering the data between 3 and 10 m s^{-1}, both the C_{D10n}, and u_* data showed a change in slope at about 6 m s^{-1} (Figs. 10b and 11b); C_{D10n} continued to decrease from 10 m s^{-1} down to a minimum value of 1.02×10^{-3} at 6 m s^{-1}. In agreement with Anderson (1993), or Smith (1980, hereafter S80), the constant value for C_{D10n} suggested by Large and Pond (1981, 1982, hereafter LP) was not found. At wind speeds below 6 m s^{-1} C_{D10n} increased, most markedly in the *Discovery* results. It has already been noted above that,

at ~6 m s^{-1} wind speed, our imbalance term ϕ_D changes sign and also that the airflow is thought to become fully turbulent (Wu 1980). That the change in nature of the results was not caused by the form of our derived ϕ_D function is shown by Fig. 13. The near-neutral *Discovery* data (for which $\phi_D = 0$) and the SOFIA data, with and without use of an imbalance correction, both exhibit a similar effect. Note that the SOFIA data processed with the assumption of zero imbalance lay below the near-neutral ($|10/L| < 0.01$) *Discovery* data. Since the SOFIA data above 5 m s^{-1} were all unstable and the small amount of data below 5 m s^{-1} were all slightly stable, the use of the imbalance terms described in section 3b showed an improved agreement between data from the two ships, particularly above the 8-m s^{-1} wind speed.

Low wind speed relationships proposed in previous studies are compared to our formulas in Figs. 12b,c. That of Trenberth et al. (1989) for winds below 3 m s^{-1} was based on an empirical fit to the low wind speed data of Dittmer (1977), Schacher et al. (1981), and LP. For low wind speeds, the Smith (1988, hereafter S88) relationship is based on formulas for the flow over an aerodynamically smooth surface. On the other hand, Wu (1994) proposed that the sea surface is aerodynamically rough at low winds. For the *Discovery* data between 3 and 6 m s^{-1}, the Wu (1994) curve is closest to our mean values. However, comparison with the SOFIA data (Fig. 12c) suggests that, on average, the *Discovery* data at these lowest wind speeds may have been biased high. If so, the S88 formula would be more appropriate, at least down to the 4 m s^{-1} wind speed.

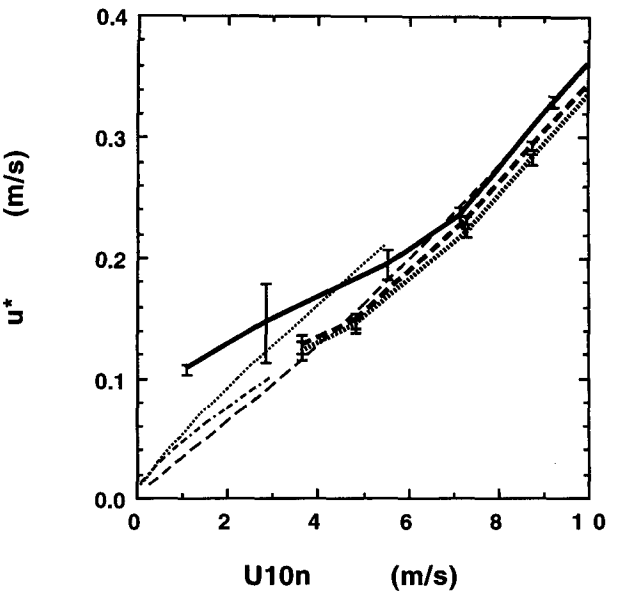

FIG. 13. Friction velocity results against 10-m neutral wind speed for low wind speeds: *Le Suroit* data with assumption of zero imbalance (dotted), *Le Suroit* data with imbalance terms (dashed), and *Discovery* near-neutral ($|10/L| < 0.01$) data (solid). Error bars indicate standard deviation of the mean. Previous low wind formulae are also shown: Wu 1994 (thin dotted), Trenberth et al. 1989 (thin chain), and Smith 1988 (thin dashed).

2) MODERATE TO HIGH WIND SPEEDS

The C_{D10n} to U_{10n} relationship for wind speeds greater than 6 m s^{-1} [Eq. (20a)] is compared in Fig. 12a with relationships proposed in previous studies. Until now LP and S80 were the major sources of wind stress data obtained at high wind speeds over the open ocean (Table 1). The relationship of Anderson (1993) is not shown in Fig. 12a since it is similar to S80. The theoretical relationship of S88 was based on the Charnock (1955) relationship (see section 4c) at moderate and high wind speeds and is seen to have a lower slope than any of the empirical relationships. The Smith et al. (1992) result for fully developed waves was inferred from a wind stress to wave-age relationship determined during the HEXMAX experiment from data obtained over relatively shallow water (18-m depth). Smith et al. (1992) agrees reasonably well with the relationship from this study. Makin et al. (1995) have also proposed a sea-state-dependent formulation for the drag coefficient. They predicted a range of results for fully developed waves, since the formulation was sensitive to the dependence of the high wavenumber tail on wave age, which is not known. Their range of results are not shown in Fig. 12a but would all lie above the results from the *Discovery*.

In comparison to S80 or LP, the relationship proposed in this study has a slightly greater slope. The mean drag coefficient is in reasonable agreement with S88 between 5 and 10 m s^{-1}, but becomes significantly greater above 15 m s^{-1}. Considering the effect of possible measurement errors in our data (Yelland et al. 1994), an underestimate in the true wind speed of about 5% would bring the results from this study into close agreement with those of S80 and LP. An error of this size is not impossible but is considered unlikely since the anemometer site was high up and well forward on the bow of the ship.[1]

Alternatively, Smith et al. (1992) suggested that the eddy correlation results from S80 may be low "by a few percent" due to possible flow distortion, which was in addition to effects resulting from the tilt of the platform (which was used simultaneously by LP). In both S80 and LP the relatively few eddy correlation measurements obtained for winds over 15 m s^{-1} (24

[1] However, we have recently obtained preliminary results from computer modeling of the airflow around ships that show that although the error in the mean wind speed may be small, the lifting of the airflow over the bows of a ship may be significant. This would reduce the measured drag coefficient and bring the *Discovery* results closer to those of Smith (1980).

and 36 values, respectively) tended to lie above their mean C_{D10n} to U_{10n} relationships. Large and Pond extended the wind speed range of their relationship by using a large number of data obtained with the dissipation method, which had, in effect, been calibrated against the lower wind speed eddy correlation data. The stability range of the LP data was large ($-0.6 < z/L < 0.15$), and the mean relationship may have been increased significantly if the analysis had included an imbalance term of the form proposed in this study. Indeed, if the data from this study is processed without the use of an imbalance term, and data from all stabilities are included in the calculation of a mean relationship, then the result is very similar to that of S80 and LP. Note, however, that the neutral data would not be changed and would now lie above the mean relationship. It must be stressed that our higher values are not a result of the imbalance term overcorrecting nonneutral data, since very near-neutral data ($|10/L| < 0.005$) is present to 20 m s^{-1} and is in excellent agreement with the mean results. It is therefore suggested that both the LP and Anderson (1993) results may be low on average due to the inclusion of nonneutral data in the calculation of the mean relationship together with the assumption of zero imbalance.

3) Implications for wave effects on wind stress

It is noteworthy that the empirical relationships derived from the data in this and previous studies all show greater slopes than would be expected from a Charnock formulation such as S88 (Fig. 12a). The recent theoretical relationship of Makin et al. (1995) also predicts a greater increase than that shown by the Charnock relation. Figure 10a shows that the drag coefficient derived from a Charnock (1955) relationship

$$z_0 = \alpha u_*^2/g, \qquad (22)$$

with a Charnock constant α of 0.011 a good fit to the data between 6 and 13 m s^{-1}: this is essentially the S88 formula for that wind speed range. However, larger constants are needed at higher winds, reaching a value of 0.017 for winds over 20 m s^{-1}. In his review of wind stress studies, Wu (1980) also noted that the value of the Charnock constant seemed to depend on the wind speed range in this manner. He suggested a refinement to the Charnock relationship where the stress is modified by a viscosity and surface tension term independent of the sea state. However, our data suggest that the exact form of the resulting power law, as proposed by Wu, is very sensitive to the way the data are averaged. This will be discussed in a future paper.

Since the Charnock relationship is normally taken to refer to a fully developed sea, it might be questioned whether the departure from the Charnock relationship seen in our data was due to sea state effects. A Ship Borne Wave Recorder (SBWR) was operated on *Discovery* during the Southern Ocean cruises. The average measured significant wave height H_s is shown in Fig. 14 as a function of U_{10n}. The data used corresponded in time to the stress measurements used in this study except that data from periods when *Discovery* was moving at more than 2.0 m s^{-1} (and the SBWR data was therefore unreliable) have been excluded. Also shown in Fig. 14 is the relationship for fully developed waves based on a Pierson–Moscowitz spectrum (Bouws 1988). The apparent overdevelopment of the waves for winds below 13 m s^{-1} is caused by the inclusion of swell when calculating H_s from the one-dimensional SBWR spectra. Any state of wave development could, in fact, be present at these wind speeds.

For higher wind speeds the H_s values shown in Fig. 14 suggest that, on average, the sea state was underdeveloped. It is tempting, but erroneous, to suggest that the observed higher mean stress values (compared for example to S88) were due to this underdeveloped sea state. To investigate this, our data were separated into over- and underdeveloped sea state cases by comparison with the Bouws (1988) relationship. The C_{D10n} to U_{10n} relationships for both are shown in Fig. 15. It can be seen that there is no significant difference between either of these relationships and that from the entire dataset. Thus, the apparent variations in sea state appear to have had negligible influence on our wind stress data.

Some studies (e.g., Geernaert et al. 1986; Denman and Miyake 1973; Large and Pond 1981) have suggested that the effects of varying sea state could cause

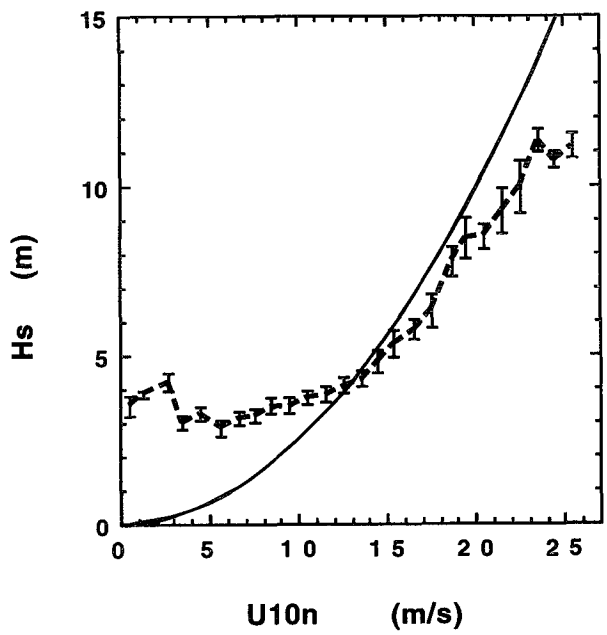

FIG. 14. Mean significant wave height (H_s) data from the Ship Borne Wave Recorder. Solid line indicates the H_s expected for fully developed seas.

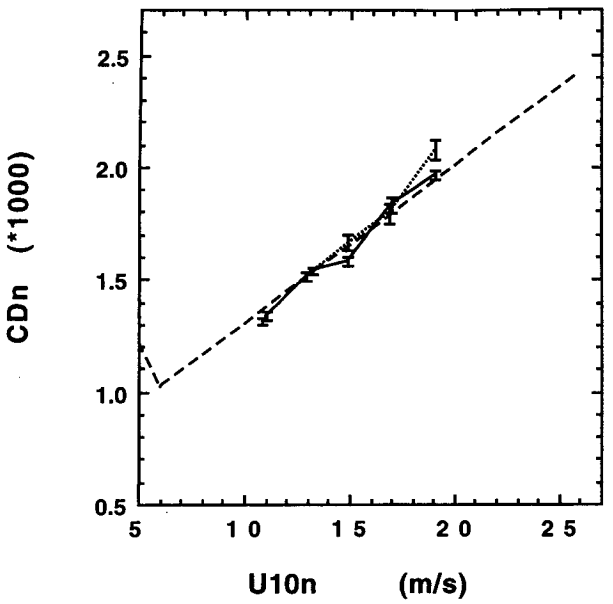

FIG. 15. Mean drag coefficient results for underdeveloped waves (solid line) and overdeveloped waves (dotted), compared to the fit to all data from Eq. (20a) (dashed).

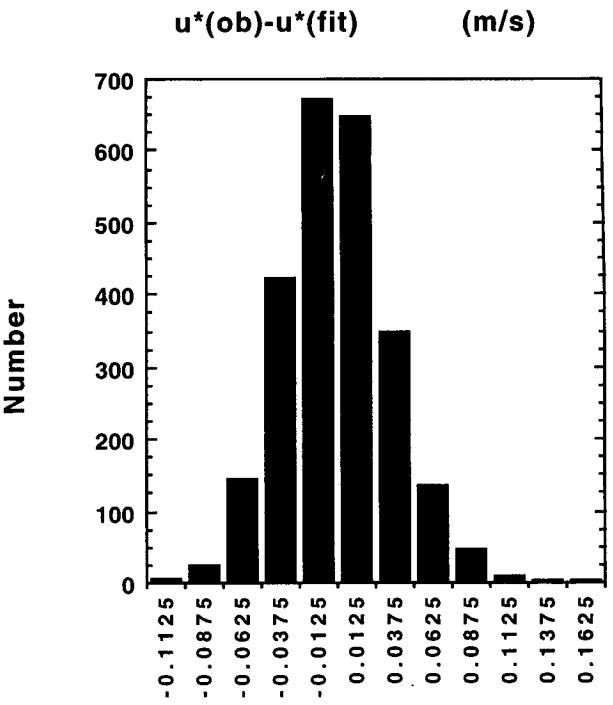

FIG. 16. (a) Histogram of absolute differences between observed value of friction velocity and that expected from Eq. (20c).

anomalies of the order of 20% in the drag coefficient over a period of a few hours. The magnitude of the scatter present in our data is summarized in Fig. 16. Ninety-eight percent of the u_* estimates were within 0.075 m s^{-1} of the mean u_* value for a given wind speed (Fig. 16a). Absolute differences are given since the variation in friction velocity appears to vary little with wind speed (Fig. 11a). In fact, the rms scatter for u_* was less than 10%, which is within the scatter to be expected due to measurement error, instrument noise, and the calculation of the true wind speed (Yelland et al. 1994). The drag coefficient results (Fig. 16b) show similar scatter to that in other studies, but we have not found significant anomalies in our data that are coherent over a few hours. Sea-state effects of the order predicted by Smith et al. (1992) or Juszko et al. (1995) are not seen. However, those effects were predicted on the basis of a pure wind-induced sea. Donelan et al. (1993) found that the relationship between drag coefficient and significant wave height obtained for wind-induced waves was obscured when the wave field was dominated by swell. It is very likely that swell dominated during the *Discovery* Southern Oceans cruises, especially at low to moderate winds. It may be that the conditions needed to detect the effects of sea state on the wind stress may occur rather infrequently over the open ocean.

It is also possible that the assumption of zero imbalance in the inertial dissipation formula may have been responsible for some of the "wave effects" seen in previous studies. If a rapid change in wind speed or direction was associated with the passage of a front, then a change in the stability conditions would often be expected, as well as a change in sea state.

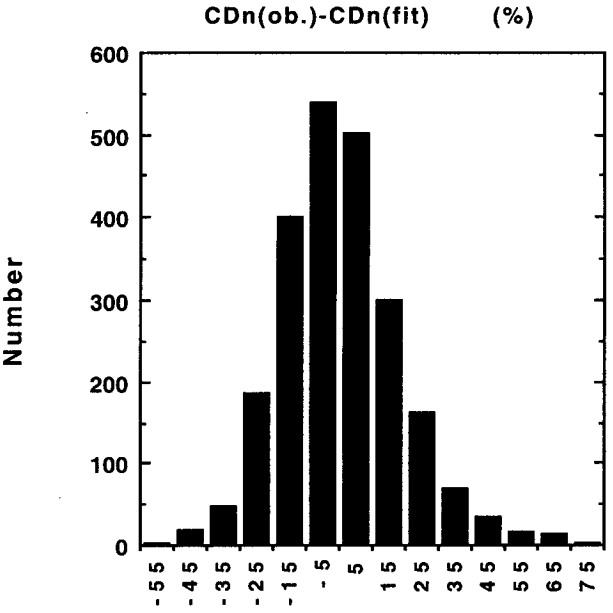

FIG. 16. (b) Scatter in drag coefficient values for wind speeds above 6 m s^{-1}: difference between observed value and that expected from Eq. (20a) expressed as a percentage of the expected value.

5. Summary

The wind stress determinations made using the inertial dissipation method from the RRS *Discovery* provide the largest amount of open ocean data to date and were obtained over a wide range of wind speeds and stabilities. This has allowed us to show that the errors incurred by assuming a balance between local production and dissipation of turbulent kinetic energy are significant even in the mean wind stress to wind speed relationship. We have suggested a form for the imbalance term which, while very tentative for stable data, is well founded for the unstable conditions that predominate over the oceans. It is a function of the wind speed and stability

$$\phi_D = \frac{z}{L}\left(2 - \frac{U_{10n}}{3}\right), \quad z/L \leq 0, \qquad (19a)$$

where U_{10n} is in meters per second. This relationship was based on the assumption of zero imbalance under neutral conditions. The implication is that, on average, local production exceeds dissipation by about 10%. However, if the true value for the Kolmogorov constant is $K = 0.52$, rather than the value $K = 0.55$ used here, then dissipation exceeds production close to neutral stability. On average, dissipation would then equal production, but neglect of the imbalance term would still result in a biased value for the derived friction velocity.

Little low wind speed data has been obtained until recently, due mainly to the problems of instrument response associated with propeller anemometers. The sonic anemometer used was not affected in this way but was situated at some height (18.5 m) from the sea surface. However, the C_{D10n} to U_{10n} relationship for wind speeds between 3 and 6 m s^{-1}

$$1000C_{D10n} = 0.29 + \frac{3.1}{U_{10n}} + \frac{7.7}{U_{10n}^2}$$

predicts values of the drag coefficient similar to Wu (1980) and is a good fit to the results of Geernaert et al. (1988).

For wind speeds greater than 6 m s^{-1}, the mean relationship

$$1000C_{D10n} = 0.60 + 0.070U_{10n}$$

is recommended for open ocean conditions. It is suggested that the higher C_{D10n} values predicted at higher wind speeds, compared for example to the open ocean measurements of Large and Pond (1981, 1982), are due to the previous authors neglect of the imbalance term in the turbulent kinetic energy budget. It is noted that all the open ocean datasets show a greater increase of C_{D10n} with wind speed than would be predicted by the Charnock formula. Wave observations suggest that, for our data at these higher wind speeds, the sea state was not fully developed. However, our C_{D10n} to U_{10n} relationship is similar to that proposed by Smith et al. (1992) for fully developed seas, and our results do not vary significantly with the mean state of wave development.

For a given wind speed the rms scatter in u_* was less than 10%, which is within the scatter to be expected due to the various measurement errors. It was not possible to detect any significant drag coefficient anomalies despite the wide range of conditions encountered. This suggests that, over the open ocean, the effects of sea state on wind stress may not be as large or frequent as sometimes suggested.

Acknowledgments. We appreciate the work of Keith Birch, Robin Pascal, Charles Clayson, and Paul Smith of the COTD team in preparing the meteorological instruments and software. This research was partly funded by the Ministry of Agriculture, Fisheries and Food.

REFERENCES

Anderson, R. J., 1993: A study of wind stress and heat flux over the open ocean by the inertial dissipation method. *J. Phys. Oceanogr.*, **23,** 2153–2161.

Birch, K. G., and R. W. Pascal, 1987: A meteorological system for research applications—MultiMet. *Fifth Int. Conf. on Electronics for Ocean Technology,* Edinburgh, Scotland, Institute of Electronic and Radio Engineers, 7–12.

Blanc, T. V., 1985: Variation of bulk derived surface flux, stability, and roughness results due to the use of different transfer coefficient schemes. *J. Phys. Oceanogr.*, **15,** 650–669.

Bouws, E., 1988: Basic definitions and descriptions of ocean waves. *Guide to Wave Analysis and Forecasting.* World Meteorological Society Publ. 702, 23–25.

Busch, N. E., 1972: On the mechanics of atmospheric turbulence. *Workshop on Micrometeorology,* D. A. Haugen, Ed., Amer. Meteor. Soc., 1–65.

Charnock, H., 1955: Wind stress on a water surface. *Quart. J. Roy. Meteor. Soc.*, **81,** 639–640.

Deacon, E. L., 1988: The streamwise Kolmogoroff constant. *Bound.-Layer Meteor.*, **42,** 9–17.

Denman, K. L., and M. Miyake, 1973: Behavior of the mean wind, the drag coefficient, and the wave field in the open ocean. *J. Geophys. Res.*, **78,** 1917–1931.

Dittmer, K., 1977: The hydrodynamic roughness of the sea surface at low wind speeds. *Meteor. Forsch. Ergebn.*, **12,** 10–15.

Donelan, M., 1990: Air–Sea Interaction. Vol. 9. *The Sea: Ocean Engineering Science,* I. M. Hanes, Ed., Wiley and Sons, 239–292.

——, F. Dobson, S. D. Smith, and R. A. Anderson, 1993: On the dependence of sea surface roughness on wave development. *J. Phys. Oceanogr.*, **23,** 2143–2149.

Dunckel, M., L. Hasse, L. Krugermeyer, D. Schriever, and J. Wucknitz, 1974: Turbulent fluxes of momentum, heat and water vapour in the atmospheric surface layer at sea during ATEX. *Bound.-Layer Meteor.*, **6,** 81–106.

Dupuis, H., A. Weill, K. Katsaros, and P. K. Taylor, 1995: Turbulent heat fluxes by profile and inertial dissipation methods: Analysis of the atmospheric surface layer from shipboard measurements during the SOFIA/ASTEX and SEMAPHORE experiments. *Ann. Geophys.*, **13,** 1065–1074.

Edson, J. B., C. W. Fairall, P. G. Mestayer, and S. E. Larsen, 1991: A Study of the inertial-dissipation method for computing air–sea fluxes. *J. Geophys. Res.*, **96**(C6), 10 689–10 711.

Fairall, C. W., and S. E. Larsen, 1986: Inertial-dissipation methods and turbulent fluxes at the air–ocean interface. *Bound.-Layer Meteor.*, **34,** 287–301.

——, and J. B. Edson, 1994: Recent measurements of the dimensionless turbulent kinetic energy dissipation function over the ocean. *Second Int. Conf. on Air–Sea Interaction and on the Meteorology and Oceanography of the Coastal Zone,* Lisbon, Portugal, Amer. Meteor. Soc., 224–225.

——, ——, S. E. Larsen, and P. G. Mestayer, 1990: Inertial-dissipation air–sea flux measurements: A prototype system using realtime spectral computations. *J. Atmos. Oceanic Technol.,* **7,** 425–453.

Frenzen, P., and C. A. Vogel, 1992: The turbulent kinetic energy budget in the atmospheric surface layer: A review and an experimental reexamination in the field. *Bound.-Layer Meteor.,* **60,** 49–76.

——, and ——, 1994: On the sensitivity of the ϕ_m function to k: A corrected illustration for the turbulent kinetic energy budget in the ASL. *Bound.-Layer Meteor.,* **68,** 439–442.

Garratt, J. R., 1977: Review of drag coefficients over oceans and continents. *Mon. Wea. Rev.,* **105,** 915–929.

Geernaert, G. L., 1987: On the importance of the drag coefficient in air–sea interactions. *Dyn. Atmos. Oceans,* **11,** 19–38.

——, and W. J. Plant, 1990: *Current Theory.* Vol. 1, *Surface Waves and Fluxes.* Kluwer Academic, 336 pp.

——, K. B. Katsaros, and K. Richter, 1986: Variation of the drag coefficient and its dependence on sea state. *J. Geophys. Res.,* **91**(C6), 7667–7679.

——, S. E. Larsen, and F. Hansen, 1987: Measurements of the wind stress, heat flux, and turbulence intensity during storm conditions over the North Sea. *J. Geophys. Res.,* **92**(C12), 13 127–13 139.

——, K. L. Davidson, S. E. Larsen, and T. Mikkelsen, 1988: Wind stress measurements during the tower ocean wave and radar dependence experiment. *J. Geophys. Res.,* **93**(C11), 13 913–13 923.

Hicks, B. B., and A. J. Dyer, 1972: The spectral density technique for the determination of eddy fluxes. *Quart. J. Roy. Meteor. Soc.,* **98,** 838–844.

Juszko, B.-A., R. F. Marsden, and S. R. Waddell, 1995: Wind stress from wave slopes using Phillips equilibrium theory. *J. Phys. Oceanogr.,* **25,** 185–203.

Large, W. G., 1979: The turbulent fluxes of momentum and sensible heat over the sea during moderate to strong winds. Ph.D. thesis, University of British Columbia, 180 pp.

——, and S. Pond, 1981: Open ocean momentum flux measurements in moderate to strong winds. *J. Phys. Oceanogr.,* **11,** 324–336.

——, and ——, 1982: Sensible and latent heat flux measurements over the ocean. *J. Phys. Oceanogr.,* **12,** 464–482.

——, and J. A. Businger, 1988: A system for remote measurements of the wind stress over the oceans. *J. Atmos. Oceanic Technol.,* **5,** 274–285.

Makin, V. K., V. N. Kudryavstev, and C. Mastenbroek, 1995: Drag of the sea surface. *Bound.-Layer Meteor.,* **73,** 159–182.

Marsden, R. F., G. A. McBean, and B. A. Proctor, 1993: Momentum and sensible heat fluxes calculated by the dissipation technique during the Ocean Storms Project. *Bound.-Layer Meteor.,* **63,** 23–38.

Paulson, C. A., 1970: The mathematical representation of wind speed and temperature profiles in the unstable atmospheric surface layer. *J. Appl. Meteor.,* **9,** 857–861.

Pond, S., W. G. Large, M. Miyake, and R. W. Burling, 1979: A gill twin propeller–vane anemometer for flux measurements during moderate and strong winds. *Bound.-Layer Meteor.,* **16,** 351–364.

Schacher, G. E., K. L. Davidson, T. Houlihan, and C. W. Fairall, 1981: Measurements of the rate of dissipation of turbulent kinetic energy, ϵ, over the ocean. *Bound.-Layer Meteor.,* **20,** 321–330.

Schmitt, K. F., C. A. Friehe, and C. H. Gibson, 1978: Sea surface stress measurements. *Bound.-Layer Meteor.,* **15,** 215–228.

Smith, S. D., 1980: Wind stress and heat flux over the ocean in gale force winds. *J. Phys. Oceanogr.,* **10,** 709–726.

——, 1988: Coefficients for sea surface wind stress, heat flux and wind profiles as a function of wind speed and temperature. *J. Geophys. Res.,* **93,** 15 467–15 474.

——, R. J. Anderson, W. A. Oost, C. Kraan, N. Maat, J. DeCosmo, K. B. Katsaros, K. L. Davidson, K. Bumke, L. Hasse, and H. M. Chadwick, 1992: Sea surface wind stress and drag coefficients: The HEXOS results. *Bound.-Layer Meteor.,* **60,** 109–142.

Stull, R. B., 1988: *An Introduction to Boundary Layer Meteorology.* Kluwer Academic, 666 pp.

Trenberth, K. E., G. L. Large, and J. G. Olson, 1989: The effective drag coefficient for evaluating wind stress over the oceans. *J. Climate,* **2,** 1507–1516.

Wu, J., 1980: Wind stress coefficients over the sea surface near neutral conditions—A revisit. *J. Phys. Oceanogr.,* **10,** 727–740.

——, 1994: The sea surface is aerodynamically rough even under light winds. *Bound.-Layer Meteor.,* **69,** 149–158.

Wyngaard, J. C., 1973: On surface layer turbulence. *Workshop on Micrometeorology,* D. A. Haugen, Ed., Amer. Meteor. Soc., 136.

——, and O. R. Coté, 1971: The budgets of turbulent kinetic energy and temperature variances in the atmospheric surface layer. *J. Atmos. Sci.,* **28,** 190–201.

Yelland, M. J., P. K. Taylor, I. E. Consterdine, and M. H. Smith, 1994: The use of the inertial dissipation technique for shipboard wind stress determination. *J. Atmos. Oceanic Technol.,* **11,** 1093–1108.